

The dark matter density profile and its central behaviour in the accretion-driven scenario

Eduard Salvador-Solé¹, Alberto Manrique¹,
Guillermo González-Casado², and Steen H. Hansen³

¹ *Departament d'Astronomia i Meteorologia, and Institut de Ciències del Cosmos (UB/IEEC) associated with the Instituto de Ciencias del Espacio (CSIC), Universitat de Barcelona, Spain*

² *Departament de Matemàtica Aplicada II, Universitat Politècnica de Catalunya, Spain*

³ *Dark Cosmology Centre, Niels Bohr Institute, University of Copenhagen, Denmark*

ABSTRACT

We describe how the density profile of relaxed, spherically symmetric halos emanates from the properties of standard cold dark matter (CDM). Its collisionless nature causes the mass distribution to be smooth, while the slow rate at which accretion proceeds guarantees the inside-out growth of halos. The combined effect is that halos permanently adapt their mass distribution to the boundary condition imposed by the *current* accretion. As a consequence the characteristic density profile of relaxed halos of a given mass is determined by the CDM power spectrum through the typical accretion rate in the particular cosmology considered. This fully supports the model proposed by Manrique et al. (2003), which is also shown to be in good agreement with the results of numerical simulations. In this paper we present the predictions of this model beyond the range of present-day simulations. We show that the central asymptotic logarithmic slope depends crucially on the shape of the power spectrum of density perturbations: it is equal to a constant negative value for power-law spectra, and has central cores for the standard CDM power spectrum. The predicted density profile in the CDM case is well fit by the Sérsic profile over at least ten decades in halo mass. The values of the Sérsic parameters depend on the mass of the structure considered. A practical procedure is provided that allows one to infer the typical values of the best NFW or Sérsic fitting law parameters for halos of any mass and redshift in any given standard CDM cosmology.

Subject headings: cosmology: theory – dark matter – galaxies: halos

1. INTRODUCTION

The universal shape of the spherically averaged density profile of relaxed dark halos in high-resolution N -body simulations is considered one of the major predictions of standard Cold Dark Matter (CDM) cosmologies. Down to one percent of the virial radius R , it is well fit by the so-called NFW profile (Navarro et al. 1996, 1997)

$$\rho(r) = \frac{\rho_c r_s^3}{r(r_s + r)^2}. \quad (1)$$

For halos of a given mass M , this is specified by only one free parameter, namely the scale radius

r_s or equivalently the concentration $c \equiv r_s/R$. At radii smaller than one percent of the virial radius, however, the behavior of the density profile is unknown. Based on recent numerical simulations, some authors advocate a central asymptotic slope significantly steeper (Moore et al. 1998; Jing & Suto 2000) or shallower (Taylor & Navarro 2001; Ricotti 2003; Hansen & Stadel 2006) than that of the NFW law. Others suggest an ever decreasing absolute value of the logarithmic slope (Power et al. 2003; Navarro 2004; Reed et al. 2005), which might tend to zero as a power of the radius like in the Sérsic (1968) law (Merritt et al. 2005).

The origin of such a universal profile is poorly understood. Two extreme points of view have been envisaged. In one of these, it would be the result of significant mergers (Syer & White 1998; Raig et al. 1998; Subramanian, Cen & Ostriker 2000; Dekel, Devor & Hetzroni 2003), while in the other it would be caused by smooth accretion (Avila-Reese et al. 1998; Nusser & Sheth 1999; Del Popolo et al. 2000; Kull 2000; Manrique et al. 2003; Williams et al. 2004; Ascasibar et al. 2004).

In the merger-driven scenario, the fact that less massive halos have larger concentrations is interpreted as reflecting that they form earlier when the mean cosmic density was higher (Navarro et al. 1997). More specifically, the $M - c$ relation at $z = 0$ is consistent (Salvador-Solé et al. 1998, hereafter SSM; Wechsler et al. 2002; Zhao et al. 2003a) with the idea that all halos form through major mergers with similar values of c , which decreases during the subsequent accretion phase. The effect is as if halos were growing from the inside out, that is, by keeping r_s unaltered while R stretches according to the increase in M . N -body simulations confirm the inside-out growth of halos during slow accretion (Salvador-Solé et al. 2005; Lu et al. 2005; Romano-Diaz et al. 2006), which supports this merger-driven scenario.

In comparison, the accretion-driven scenario is at least as attractive. Manrique et al. (2003, hereafter MRSSS) showed that the inside-out growth during accretion leads to a typical density profile that appears roughly to have the NFW shape with the correct $M - c$ relation in any epoch and cosmology analyzed. Certainly, the effects of major mergers cannot be neglected in hierarchical cosmologies, however, as noted by MRSSS, if the density profile were set by the boundary conditions imposed by *current* accretion, then it would be independent of the past aggregation history of the halo, and halos could be assumed to grow by pure accretion without any loss of generality. Simultaneously this would explain why halos with very different initial conditions and aggregation histories have similar density profiles (Romano-Diaz et al. 2006).

Both the merger-driven and the accretion-driven scenarios can fit the $M - c$ relation at $z = 0$, but the difference between the two scenarios becomes progressively larger at higher redshifts. It was shown in MRSSS that only the predictions

of the accretion-driven scenario are in agreement with data from numerical simulations.

In the present paper, we show that the accretion-driven scenario is also sound from a theoretical point of view. This renders its predictions beyond the range of current simulations more reliable. Such predictions are examined in detail below.

The paper is organized as follows. In Section 2, we show how the MRSSS model emerges from the properties of standard CDM. The behavior of the predicted density profile at extremely small radii and for a wide range of halo masses is investigated in Section 3. Our results are summarized in Section 4.

2. CDM properties and halo density profile

2.1. Inside-out growth during accretion

We now argue that accretion is always slow enough for halos to grow inside-out, which, as shown in Section 2.2, has important consequences for the inner structure of these objects.

Schematically, one may distinguish between minor and major mergers. In minor mergers, the relative mass increase produced, $\Delta \equiv \Delta M/M$, is so small that the system is left essentially unaltered, whereas in major mergers Δ is large enough to cause rearrangements.

The smaller Δ , the most frequent are mergers (Lacey & Cole 1993). For this reason, although individual minor mergers do not affect the structure of halos, their added contribution yields a *smooth* secular mass increase, the so-called accretion, with apparent effects on the aggregation track $M(t)$ of the halo. The accretion scaled rate, $\dot{M}/M(t)$, is given by (Raig et al. 2001, hereafter RGS)

$$\mathcal{R}_a(M, t) = \int_0^{\Delta_m} d\Delta \Delta \mathcal{R}_m(M, t, \Delta), \quad (2)$$

where $\mathcal{R}_m(M, t, \Delta)$ is the usual Lacey-Cole (1993) instantaneous merger rate (see eq. [A1]) and Δ_m is the maximum value of Δ for mergers contributing to the accretion. In contrast major mergers are rare events yielding notable sudden mass increases or *discontinuities* in $M(t)$.

After undergoing some major merger (and virializing), halos evolve as relaxed systems until the next major merger. The fact that standard CDM

is *non-decaying and non-self-annihilating*¹ guarantees that the mass collected during such periods is conserved. This does not yet imply that halos grow inside-out during accretion, because their mass distribution might still vary owing to energy gains or losses or to the action of accretion itself. Even if each individual minor merger would leave the halo unchanged their collective action might alter these systems. However, standard CDM is also *dissipationless* and therefore halos cannot lose energy. Furthermore, under the assumption of spherical symmetry halos cannot suffer tidal torques from surrounding matter, and hence the surrounding matter is unable to alter the kinetic energy of the halo. Therefore, the only possibility for a time-varying inner mass distribution of accreting halos is that the accretion process causes it itself.

This possibility, that the process of accretion itself could alter the internal mass distribution would be realized only if the accretion time $1/\mathcal{R}_a$, were smaller than the dynamical time τ_{cr} . On the contrary, if $1/\mathcal{R}_a$ is substantially larger than τ_{cr} , the adiabatic invariance of the inner halo structure will be guaranteed, and the halo will evolve inside-out. Thus, by requiring $1/\mathcal{R}_a$ to be C times larger than τ_{cr} , we are led to the equation

$$C \left[\frac{4\pi}{3} G \Delta_{\text{vir}}(t) \bar{\rho}(t) \right]^{1/2} = \mathcal{R}_a(M, t), \quad (3)$$

which gives the upper mass M_a for inside-out growth at t . In equation (3), $\bar{\rho}$ is the mean cosmic density and $\Delta_{\text{vir}}(t)$ is the virialization density contrast given e.g. by Bryan & Norman (1998). M_a is indeed an upper limit because $\mathcal{R}_a(M, t)$ is an increasing function of t ; see RGS. In any CDM cosmology analyzed, equation (3) appears to have no solution for C significantly larger than unity in the relevant redshift range. This means that accretion is always slow enough for halos to grow inside-out as assumed in the MRSSS model.

2.2. The boundary condition imposed by accretion

Standard CDM is *collisionless* and hence free-streaming. As a consequence, all radial profiles in

¹Both decay and annihilation rates are extremely small for realistic dark matter particle candidates.

relaxed halos are necessarily smooth. This means that the derivative at any order is continuous. This holds in particular for the mass profile² $M(r)$, which has the following consequence.

The inside-out growth of a halo during accretion implies that the mass profile of the matter being aggregated, $M(t)$, must match exactly the part of the total mass profile, $M(r)$, which is being built at that time, by simple conversion through the definition of the instantaneous virial radius

$$R(t) = \left[\frac{3M(t)}{4\pi \Delta_{\text{vir}}(t) \bar{\rho}(t)} \right]^{1/3}. \quad (4)$$

Since minor mergers only produce tiny discontinuities, such a piece of $M(t)$ track will be well approximated by a smooth function, and, as the functions $\bar{\rho}(t)$ and $\Delta_{\text{vir}}(t)$ in equation (4) are also well approximated by smooth functions, the corresponding piece of the $M(r)$ profile will be smooth too. Thus, the piece of profile that is being built during accretion phases fulfills the right smooth condition and the system does not need to rearrange its structure.

Only when a halo undergoes a major merger and its $M(t)$ track suffers a marked discontinuity, the mass profile prior to the major merger will no longer match the piece that begins to develop after it. Since the $M(r)$ profile cannot have any discontinuity, the halo is then forced to rearrange its mass distribution (through violent relaxation) to fulfill the required smooth condition.

In other words, the mass distribution of standard CDM halos permanently adapts to the boundary condition imposed by current accretion. This causes rearrangements of the structure on the occasion of major mergers and very tiny (and negligible) ones during accretion periods.

According to this result, relaxed halos with mass M_i at time t_i accreting at the same rate \dot{M} will have the same mass profile $M(r)$. This proves that the fundamental assumption of the MRSSS model that the mass distribution of relaxed halos is fixed by their current accretion is a natural consequence of the slowly accreting, non-decaying, non-self-annihilating, dissipationless and collisionless nature of standard CDM.

²We are naturally referring to the *theoretical* mass profile given by the average over random realizations, or over time realizations as long as the halo evolves inside-out.

2.3. The MRSSS model

The mass profile of a specific halo with mass M_i at time t_i accreting at a given rate during any arbitrarily small time interval Δt around t_i is therefore simply the smooth extension of the small piece of profile being built during that interval. Unfortunately, the smooth extension of a small piece of function is hard to find in practice, so this does not allow one to infer the mass profile of real individual halos.

There is one case, however, in which such a smooth extension can readily be achieved: that of halos with M_i at t_i *accreting at the typical rate* $\mathcal{R}_a[M(t), t]$ during any arbitrarily small interval of time around t_i . In this case, the (unique) smooth extension we are looking for necessarily coincides with the smooth function $M(t)$, solution of the differential equation

$$\frac{\dot{M}}{M(t)} = \mathcal{R}_a[M(t), t] \quad (5)$$

for the boundary condition $M(t_i) = M_i$, by conversion from t to r by means of equation (4). Once the typical $M(r)$ profile is known, by differentiating it and taking into account equations (4) and (5), one is led to the *typical density profile for halos with M_i at t_i* proposed by MRSSS,

$$\rho(r) = \frac{1}{4\pi r^2} \left(\frac{\dot{M}}{\dot{R}} \right)_{t(r)} = [\Delta_{\text{vir}}(t) \bar{\rho}(t) \delta(t)]_{t(r)} \quad (6)$$

where

$$\delta(t) = \left[1 - \frac{1}{\mathcal{R}_a[M(t), t]} \frac{d \ln(\Delta_{\text{vir}} \bar{\rho})}{dt} \right]^{-1}. \quad (7)$$

From equations (6) and (7) we see that the shape of this profile is ultimately set by the cosmology and the CDM power spectrum of density perturbations through the merger rate $\mathcal{R}_m(M, t, \Delta)$ entering the typical accretion rate $\mathcal{R}_a(M, t)$ (see eqs. [A1] and [2]). This dependence is however so convoluted that the density profile (6) must be inferred numerically. Only its central asymptotic behavior can be derived analytically as will be shown in the next section.

3. Theoretical predictions

From equation (2) we see that the exact shape of the density profile in equation (6) depends on

Δ_m . This parameter marks the effective transition between minor and major mergers, and it can be determined from the empirical $M - c$ relation at some given redshift.

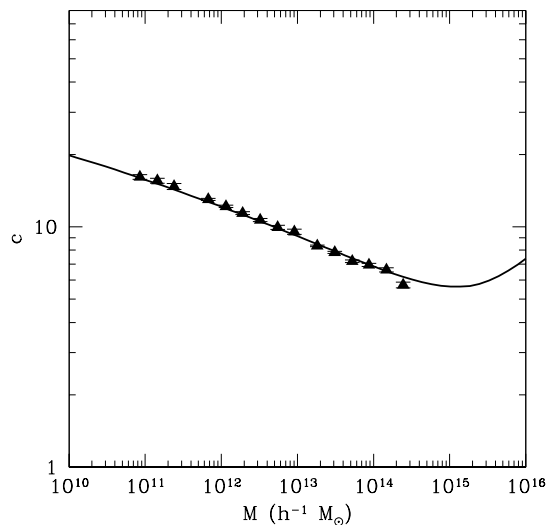


Fig. 1.— $M - c$ relation at $z = 0$ predicted in the concordance model by the MRSSS model for $\Delta_m = 0.26$ (solid line) compared to the empirical relation traced by those points with minimal error bars obtained by Zhao et al. (2003b) from high-resolution simulations (triangles with error bars).

For each given Δ_m value, the density profiles, down to $R/100$, predicted at $z = 0$ in the concordance model characterized by $(\Omega_m, \Omega_\Lambda, h, \sigma_8) = (0.3, 0.7, 0.7, 0.9)$ for halos with different masses have been fitted to the NFW profile to find the best fitting values of c . Then we searched the value of Δ_m that minimizes the departure of the theoretical $M - c$ relations from the empirical one drawn from high-resolution simulations by Zhao et al. (2003b). As shown in Figure 1, $\Delta_m = 0.26$ gives an excellent fit over almost 4 decades in mass ($8 \times 10^{10} h^{-1} M_\odot < M < 4 \times 10^{14} h^{-1} M_\odot$).

In Figure 2, we plot, down to a radius equal to the current resolution radius of most numerical simulations, the density profiles predicted in the concordance model for halo masses at $z = 0$ ranging from 10^{11} to $10^{16} M_\odot$. As expected, they are all well fit to a NFW profile although

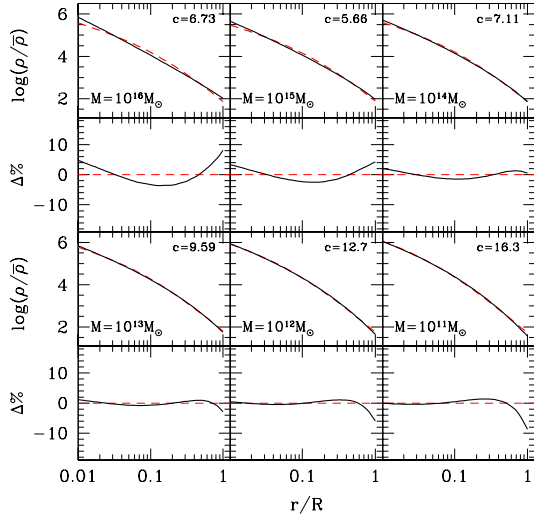


Fig. 2.— Predicted density profiles (solid lines) compared to their fits to a NFW profile (dashed lines) for halo masses at $z = 0$ ranging from $10^{16} M_{\odot}$ to $10^{11} M_{\odot}$ (or, equivalently, from 10^3 to 10^{-2} times the current critical mass $M_{\star 0}$ for collapse) in the concordance model. *Upper sections*: profiles. *Lower sections*: residuals of the logarithmic fits. The halo mass and the corresponding best-fitting value of the NFW concentration parameter are quoted in each panel.

there is the tendency for the theoretical profiles for $M \gtrsim 10^{14} M_{\odot}$ to deviate from that shape and approach a power-law with logarithmic slope intermediate between the NFW asymptotic values of -1 and -3 . This tendency also makes c increase very rapidly at large masses where the fit by the NFW law is no longer acceptable. This causes the $M - c$ relation to deviate from its regular trend at smaller M (see Fig. 2). Both effects, already reported in MRSSS, were later observed in simulated halos (Zhao et al. 2003b; Tasitsiomi et al. 2004). This is a clear indication that the NFW profile is not providing an optimal fit for very massive structures.

A useful prediction of the MRSSS model is the following. As explained in Salvador-Solé et al. (2005), the $M(t)$ tracks traced by accreting halos (hence growing inside-out) coincide with curves of

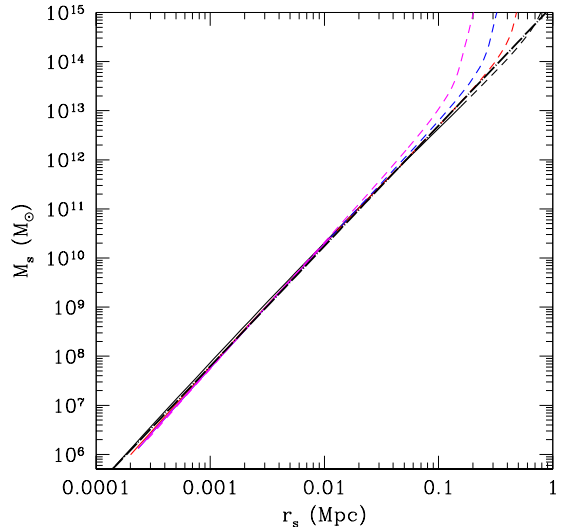


Fig. 3.— Relations between the NFW r_s and M_s parameters obtained in the concordance model (solid lines for masses up to $10M_*(z)$ and dashed lines beyond it) from the fits of the theoretical density profiles of halos with varying mass at the redshifts 0., 1.03, 2.08 and 3.94. The dot-dashed line gives the analytical fit (see text) to the mean of the solid lines.

constant r_s and M_s values, with M_s defined as the mass interior to r_s . Thus, the intersection of those accretion tracks at any arbitrary redshift sets the relation $M_s(r_s)$ between such a couple of parameters, implying that the $M_s(r_s)$ relation satisfied by halos is *time-invariant*. In Figure 3, we show how the different $M_s(r_s)$ curves obtained by fitting to a NFW law the density profiles predicted at different redshifts overlap. There is only some deviation at large masses where the density profiles are not correctly described by the NFW profile. Such a time-invariant $M_s(r_s)$ relation is well fit, for r_s in the range $10^{-4} \text{ Mpc} < r_s < 1 \text{ Mpc}$, by

$$\frac{M_s}{10^{13} M_{\odot}} = 141 \left(\frac{r_s}{\text{Mpc}} \right)^{2.45}. \quad (8)$$

Substituting equation (8) into the relation

$$\frac{M_s}{M} = \frac{\ln 2 - 0.5}{g(c)} \quad (9)$$

which holds for NFW profiles, one is led to

$$\left[\frac{4\pi \Delta_{\text{vir}}(t) \bar{\rho}(t)}{2.37 \times 10^6 \bar{\rho}_0} \right]^{0.82} \left[\frac{M}{10^{13} M_{\odot}} \right]^{0.18} = \frac{g(c)}{c^{2.45}}, \quad (10)$$

where $g(c)$ stands for $\ln(1+c) - c/(1+c)$ and $\bar{\rho}_0$ is the current mean cosmic density. The relation (10) is an implicit equation for the concentration of halos with any given mass and redshift.

What about the central behavior of the predicted density profile? According to equation (4), small radii correspond to small cosmic times. In this asymptotic regime all Friedman cosmologies approach the Einstein-de Sitter model in which $\Delta_{\text{vir}}(t)$ is constant and $\bar{\rho}(t)$ is (in the matter dominated era when halos form) proportional to t^{-2} . If the power spectrum of density perturbations were of the power-law form, $P(k) \propto k^j$ with index j satisfying $1 > j > -3$ to guarantee hierarchical clustering, then the universe would be self-similar. The mass accretion in equation (5) would take the asymptotic form: $M(t) \propto t^{\frac{2}{j+3}}$ (see the Appendix). The fact that both $\Delta_{\text{vir}}(t)\bar{\rho}(t)$ and $M(t)$ would then be power-laws has two consequences. First, the time dependences of their respective logarithmic derivatives on the right of equation (7) cancel, which implies that $\rho(t)$ is proportional to $\Delta_{\text{vir}}(t)\bar{\rho}(t)$, and hence to $\bar{\rho}(t)$. Second, the virial radius given by equation (4) is also a power-law, $R(t) \propto [M(t)/\bar{\rho}(t)]^{1/3} \propto t^{2(j+4)/[3(j+3)]}$. From this we get $t(r)$, and thereby one finds

$$\rho(r) \propto r^{-\frac{3(j+3)}{j+4}}. \quad (11)$$

This central behavior, fully in agreement with the numerical profiles obtained from power-law power spectra, is particularly robust as it does not depend on Δ_{m} . We note that for $j = 0$ one has a central slope of 2.25.

The CDM power spectrum is of course not a power-law. However, in the limit of small masses involved in that asymptotic regime, it tends to a power-law of index $j = -3$. Thus, according to the relation (11), we expect a vanishing central logarithmic slope of $\rho(r)$ for the standard CDM case. This is again confirmed by the numerical profiles obtained in this case: as one goes deeper and deeper into the halo center, they become increasingly shallower.

What is more remarkable is that down to a radius as small as 1 pc, the density profiles appear

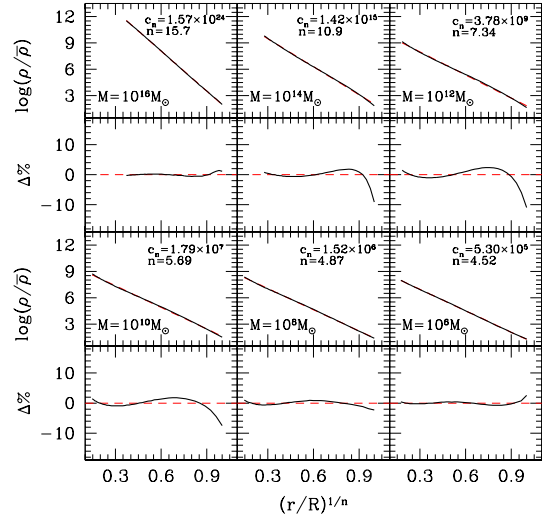


Fig. 4.— Same as Figure 2 but for the Sérsic profile. All the profiles are now drawn down to 1 pc radius and cover a wider range of halo masses: $10^{16} M_{\odot}$ to $10^6 M_{\odot}$ (or, equivalently, from 10^3 to 10^{-7} times $M_{\star 0}$).

to be well fit by the Sérsic (1968) law

$$\rho(r) = \rho_0 \exp \left[- \left(\frac{r}{r_n} \right)^{1/n} \right], \quad (12)$$

over at least 10 decades in halo mass (see Fig. 4), from $10^6 M_{\odot}$ to $10^{16} M_{\odot}$. We remind that, for power-law spectra, equation (6) leads to density profiles with central cusps, so the Sérsic shape is not a general consequence of the MRSSS model, but it is specific of the standard CDM power spectrum. In fact, from the reasoning above we see that what causes the zero central logarithmic slope in the CDM case is the fact that the logarithmic accretion rate $d \ln M(t)/d \ln t = t \mathcal{R}_a[M(t), t]$ diverges in the limit of small t . This is in contrast to the general power-law case, where the accretion rate remains finite.

Similar to the characteristic density ρ_c in the NFW profile (eq. [1]), the central density ρ_0 entering the Sérsic law (eq. [12]) can be written in terms of the mass M and the values of the two (instead of one) remaining parameters, n and r_n

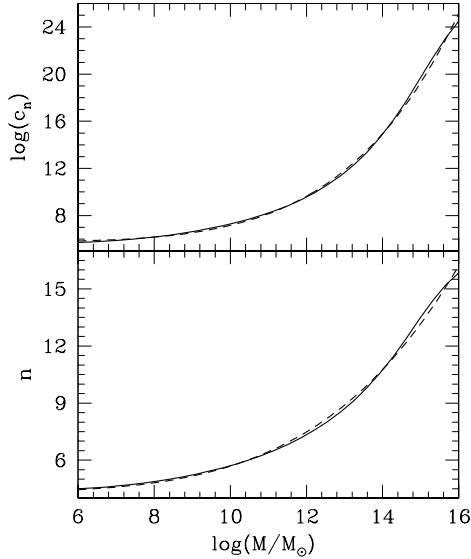


Fig. 5.— Mass dependence at $z = 0$ of the Sérsic law parameters n and c_n fitting the predicted density profiles of halos in the concordance model (full lines) and their fits by the simple expressions given in the text (dashed lines).

or $c_n \equiv R/r_n$,

$$\rho_0 = \frac{M}{4\pi n r_n^3 \Gamma(3n)} P^{-1}(3n, c_n^{1/n}), \quad (13)$$

where Γ is the usual gamma function and

$$P(a, x) = \frac{1}{\Gamma(a)} \int_0^x dt e^{-t} t^{a-1} \quad (14)$$

is the incomplete or regularized one. At $z = 0$, the two free parameters n and c_n depend on M according to the relations plotted in Figure 5, which are well approximated by

$$n(M) = 4.32 + 7.5 \times 10^{-7} \left[\ln \left(\frac{M}{M_\odot} \right) \right]^{4.6}, \quad (15)$$

$$\ln[c_n(M)] = 13.3 + 7.5 \times 10^{-8} \left[\ln \left(\frac{M}{M_\odot} \right) \right]^{5.6}, \quad (16)$$

leading to the following combined relation

$$c_n(M) = 5.84 \times 10^5 \left(\frac{M}{M_\odot} \right)^{\frac{n-4.32}{10}}. \quad (17)$$

These expressions are useful to infer the typical values of the Sérsic parameters for present-day halos with any mass. It is worth mentioning that the predicted values of n are of the same order of magnitude as the ones obtained by Merritt et al. (2005) from simulated halos with masses ranging from dwarfs galaxies to galaxy clusters (the values of c_n were not presented in that work).

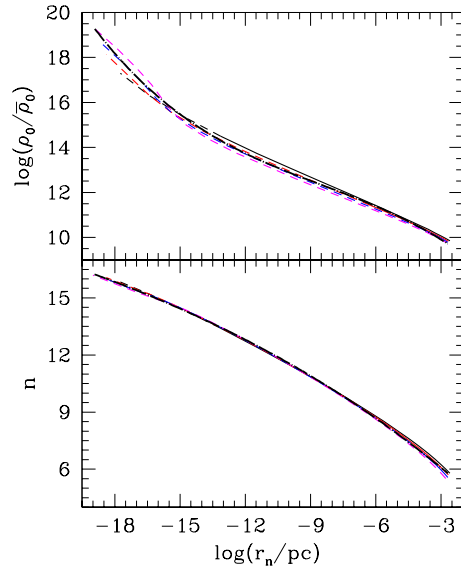


Fig. 6.— Same as Figure 3 but for the $\rho_0(r_n)$ and $n(r_n)$ relations among the best fitting Sérsic parameters. In dot-dashed lines the respective analytical fits (see text) to the mean curve. $\bar{\rho}_0$ is the current mean cosmic density.

To obtain more general values of these parameters for halos of any mass and redshift, we can proceed as in the NFW case above. For reasons identical to the ones leading to the time-invariant relation $M_s(r_s)$, the relations $\rho_0(r_n)$ and $n(r_n)$ must be time-invariant. In Figure 6, we see how the corresponding curves obtained from the fit to the Sérsic profile of the same density profiles as used in Figure 3 overlap, indeed, even better than the $M_s(r_s)$ curves do, since there is no large deviations at large masses. These invariant relations are well fit, for $x \equiv \log(r_n/\text{Mpc})$ in the range

$-25 < x < -9$, by

$$\begin{aligned} \rho_0(r_n) &= \bar{\rho}_0 \exp(A), \\ A &= -2.48 - 4.73x \\ &\quad - 0.270x^2 - 6.24 \times 10^{-3}x^3, \end{aligned} \quad (18)$$

$$\begin{aligned} n(r_n) &= -4.43 - 1.43x \\ &\quad - 0.0313x^2 - 2.98 \times 10^{-4}x^3. \end{aligned} \quad (19)$$

Replacing these expressions into equation (13), we can solve for r_n and then use the relation (19) to find the value of n .

4. Summary

We have described how the universal density profile of relaxed halos emanates from the basic properties of standard CDM. In doing so, we have justified the accretion-driven model for the density profile of halos proposed by MRSSS, which was previously shown to be in overall agreement with the results of numerical simulations. In this scenario the density profile of relaxed halos is simply the analytical extension of the piece of profile currently building up through accretion. The typical shape of the density profile in any given cosmology is set by the mass and typical accretion rate of the halo.

The MRSSS model makes specific predictions for the central asymptotic behavior of the halo density profile, which depends on the power spectrum of density perturbations. The prediction made in the case of power-law spectra can be readily checked by means of numerical simulations provided one concentrates on massive halos as these reached the asymptotic regime at larger radii. In the case of the standard CDM power spectrum, the model predicts a vanishing central logarithmic slope. The way this asymptotic behavior is reached is surprisingly simple: down to a radius as small as 1 pc, the density profile is well fit by the Sérsic profile over at least 10 decades in halo mass.

Another prediction of the MRSSS model with useful practical applications is the existence of time-invariant relations among the NFW or Sérsic law parameters (M_s and r_s in the former case and ρ_0 , r_n and n in the latter) fitting the halo density profiles. A code is publicly available at <http://www.am.ub.es/cosmo/gravitation.html>

that computes such invariant relations for any desired standard CDM cosmology.

Finally, let us note that, although halos have been assumed to be spherically symmetric throughout the present paper, this is not crucial for the MRSSS model. As shown in a following paper (González-Casado et al. 2007), the results presented here also hold for more realistic triaxial rotating halos. Furthermore, an approach similar to the one followed here allows one to explain not only their mass distribution, but also other of their structural and kinematical properties, such as the radial dependence of angular momentum.

This work was supported by the Spanish DGES grant AYA2003-07468-C03-01. We thank Donghai Zhao and co-workers for kindly providing their data.

REFERENCES

- Ascasibar Y., Yepes G., Gottlöber S., Müller, V., 2004, MNRAS, 352, 1109
- Avila-Reese V., Firmani C., Hernández X., 1998, ApJ, 505, 37
- Bryan G. L., Norman M. L., 1998, ApJ, 495, 80
- Cohn, J. D., White, M., 2005, APh, 24,316
- Dekel A., Devor J., & Hetzroni G., 2003, MNRAS, 341, 326
- Del Popolo A., Gambera M., Recami E., Spedicato, E., 2000, A&A, 353, 427
- Hansen S. H., Stadel J., 2006, JCAP, 0605, 014 [arXiv:astro-ph/0510656].
- González-Casado, G., Salvador-Solé, E., Manrique, A., Hansen, S., 2007, to appear.
- Jing Y. P., Suto Y., 2000, ApJ, 529, L69
- Jing, Y. P. 2000, ApJ, 535, 30
- Kull A., 2000, ApJ, 516, L5
- Lacey C., Cole S., 1993, MNRAS, 262, 627
- Lu Y, Mo H. J., Katz N., Wienberg M. D., 2005, MNRAS, 368, 1931
- Manrique A., Raig A., Salvador-Solé E., Sanchis T., Solanes J. M., 2003, ApJ, 593, 26 (MRSSS)

- Merritt D., Navarro J. F., Ludlow A., Jenkins A., 2005, ApJ, 624, L85
- Moore B., Governato F., Quinn T., Stadel J., Lake G., 1998, ApJ, 490, 493
- Moore B., Quinn T., Governato F., Stadel J., Lake G., 1999, MNRAS, 310, 1147
- Navarro J. F., 2004, MNRAS, 349, 1039
- Navarro J. F., Frenk C. S., White S. D. M., 1996, ApJ, 462, 563
- Navarro J. F., Frenk C. S., White S. D. M., 1997, ApJ, 490, 493 (NFW)
- Nusser A., Sheth R. K., 1999, MNRAS, 303, 685
- Power C., Navarro J. F., Jenkins A., Frenk C. S., White S. D. M., Springel V., Stadel J., Quinn T., 2003, MNRAS, 338, 14
- Raig A., González-Casado G., Salvador-Solé E., 1998, ApJ, 508, L129
- Raig A., González-Casado G., Salvador-Solé E. 2001, MNRAS, 327, 939 (RGS)
- Reed D., Governato F., Verde L., Gardner J., Quinn T., Stadel J., Merrit D., Lake G., 2005, MNRAS 357, 82
- Ricotti, M., 2003, MNRAS, 344, 1237
- Romano-Diaz, E., Faltenbacher, A., Jones, D., Heller, C., Hoffman, Y., Shlosman, I., 2006, ApJ, 637, L93
- Salvador-Solé E., Manrique A., Solanes J. M., 2005, MNRAS, 358, 901
- Salvador-Solé E., Solanes J. M., Manrique A., 1998, ApJ, 499, 542 (SSM)
- Sérsic J. L., 1968, Atlas de Galaxias Australes (Córdoba: Obs. Astron., Univ. Nac. Córdoba)
- Subramanian K, Cen R., Ostriker J. P., 2000, ApJ, 538, 528
- Syer D., White S. D. M., 1998, MNRAS, 293, 337
- Tasitsiomi, A., Kratsov, A., Gottlöber, S., Klypin, A. A., 2004, 607, 125
- Taylor, J. E., Navarro, J. F., 2001, ApJ, 563, 483
- Wechsler R. H., Bullock J. S., Primack J. R., Kravtsov A. V., Dekel A., 2002, ApJ, 568, 5
- Williams L. L. R., Babul A., Dalcanton J. J., 2004, ApJ, 604, 18
- Zhao D. H., Mo H. J., Jing Y. P., Börner G., 2003a, MNRAS, 339, 12
- Zhao, D. H., Jing, Y. P., Mo, H. J., Börner, G., 2003b, ApJ, 597, L9

This 2-column preprint was prepared with the AAS L^AT_EX macros v5.2.

A. The accretion track asymptotic behavior

The instantaneous rate of mergers undergone by halos with mass M at t yielding a relative mass increase Δ is (Lacey & Cole 1993)

$$\mathcal{R}_m(M, t, \Delta) = \frac{\sqrt{2/\pi} M}{\sigma^2(M')} \left| \frac{d\delta_c}{dt} \frac{d\sigma(M')}{dM'} \right| \left[1 - \frac{\sigma^2(M')}{\sigma^2(M)} \right]^{-3/2} \exp \left\{ -\frac{\delta_c^2(t)}{2\sigma^2(M')} \left[1 - \frac{\sigma^2(M')}{\sigma^2(M)} \right] \right\}, \quad (\text{A1})$$

where $M' \equiv M(1 + \Delta)$ is the final mass, $\delta_c(t)$ is the linearly extrapolated, cosmology-dependent, critical density contrast of density fluctuations at t for collapse at the present time t_0 and $\sigma(M) \equiv \sigma(M, t_0)$ is the rms density contrast of fluctuations on scale M at t_0 , related to the zeroth order spectral moment.

In a self-similar universe with spectral index j , one has

$$\delta_c(t) = \delta_{c0} \left(\frac{t}{t_0} \right)^{-2/3}, \quad \sigma(M) = \sigma(M_{\star 0}) \left(\frac{M}{M_{\star 0}} \right)^{-\frac{j+3}{6}} \quad (\text{A2})$$

where δ_{c0} and $M_{\star 0}$ are the current values of $\delta_c(t)$ and $M_{\star}(t)$, respectively, $M_{\star}(t)$ being the critical mass for collapse at t , solution of the implicit equation $\sigma(M_{\star}, t) = \delta_{c0}$. Therefore, equation (A1) takes the form

$$\mathcal{R}_m(M, t, \Delta) = \sqrt{\frac{2}{\pi}} \frac{j+3}{9t} \frac{\nu(M, t) (1 + \Delta)^{2\frac{j+3}{3}-1}}{\left[(1 + \Delta)^{\frac{j+3}{3}} - 1 \right]^{3/2}} \exp \left\{ -\frac{\nu^2(M, t)}{2} \left[(1 + \Delta)^{\frac{j+3}{3}} - 1 \right] \right\}, \quad (\text{A3})$$

where

$$\nu(M, t) = \left(\frac{t}{t_0} \right)^{-2/3} \left(\frac{M}{M_{\star 0}} \right)^{\frac{j+3}{6}} = \left[\frac{M}{M_{\star}(t)} \right]^{\frac{j+3}{6}}. \quad (\text{A4})$$

Substituting expression (A3) in equation (2) and changing Δ by $x = \nu^2[(1 + \Delta)^{(j+3)/3} - 1]$, we obtain the following expression for the accretion rate

$$\mathcal{R}_a(M, t) = \frac{3A\nu^2}{(j+3)t} \int_0^{x_m(M, t, \Delta_m)} dx \left[(1 + \nu^{-2}x)^{\frac{3}{j+3}} - 1 \right] (1 + \nu^{-2}x) \frac{\exp(-x/2)}{x^{\frac{3}{2}}}, \quad (\text{A5})$$

where, for simplicity, we have dropped the explicit dependence of ν and used the notation $A = \sqrt{2/\pi} (j+3)/9$ and $x_m(M, t, \Delta_m) = \nu^2[(1 + \Delta_m)^{(j+3)/3} - 1]$.

In the differential equation (5), the variable M in \mathcal{R}_a is replaced by the mass accretion track $M(t)$. As halos grow through both accretion and major mergers, accretion tracks $M(t)$ increase with increasing time less rapidly than does $M_{\star}(t)$ tracing the typical mass evolution of halos in any self-similar universe. Thus, $\nu(t) \equiv \nu[M(t), t]$ is a decreasing function of t (see eq. [A4]) and, in the small t asymptotic regime, $\nu(t)^{-2}$ tends to zero. Taking the Taylor series expansion of $[1 + \nu^{-2}(t)x]^{3/(j+3)}$ inside the integral on the right of equation (A5), at leading order in $\nu^{-1}(t)$, we obtain

$$\mathcal{R}_a[M(t), t] = \frac{9At^{-1}}{(j+3)^2} \int_0^{x_m(t)} dx \frac{\exp(-x/2)}{\sqrt{x}} = \frac{9\sqrt{2\pi}At^{-1}}{(j+3)^2} \operatorname{erf} \left[\nu(t) \sqrt{(1 + \Delta_m)^{\frac{j+3}{3}} - 1} \right], \quad (\text{A6})$$

where $\operatorname{erf}(x)$ is the error function. Given the value of constant A and given that, for $\nu(t)$ tending to infinity, the error function approaches unity, we are led to

$$\mathcal{R}_a[M(t), t] = \frac{2}{j+3} t^{-1}. \quad (\text{A7})$$

Finally, integrating equation (5) for such an accretion rate, we are led to the following asymptotic behavior for accretion tracks

$$M(t) \propto t^{\frac{2}{j+3}}. \tag{A8}$$

Note how it compares with the time dependence of the critical mass in a self-similar universe: $M_*(t) \propto t^{\frac{4}{j+3}}$.